JOURNAL OF ADVANCED VETERINARY AND ANIMAL RESEARCH
ISSN 2311-7710 (Electronic)
http://doi.org/10.5455/javar.2025.l992
A periodical of the Network for the Veterinarians of Bangladesh (BDvetNET)

December 2025
VOL 12, NO. 4, PAGES 1314–1332

ORIGINAL ARTICLE

Mechanistic insights into *Calotropis procera* extract and green-silver nanoparticles as therapeutic agents in murine schistosomiasis: Targeting *BAX*/Bcl-2 and oxidative stress

Zeyad K. Hamdan[1], Muzayyan Fadhly Namik[1], Noor Adnan Mahmood[1], Mohammad I. Soliman[2], Mohammed A. Abdel-Rasol[2], Ahmed H. Nigm[2]

[1]Department of Biology, College of Education for Pure Science, Tikrit University, Tikrit, Iraq
[2]Department of Zoology, Faculty of Science, Ain Shams University, Cairo, Egypt

ABSTRACT

Objective: This study aims to make a comparative evaluation of the therapeutic efficacies of the *Calotropis* extract (CpE) and green silver nanoparticles (GSNPs) compared to praziquantel (PZQ) in treating mice infected with schistosomiasis, with a comprehensive assessment of host physiological responses.

Materials and Methods: The CpE-fabricated silver nanoparticles were characterized (UV-vis spectroscopy, transmission electron microscopy, and Fourier transform infrared). Five experimental groups were conducted: uninfected, infected untreated, PZQ-, CpE-, and GSNP-treated. The parasitological, biochemical, histopathological, and ultrastructural approaches were employed in evaluating each treatment protocol.

Results: It was found that the reduction of the worm burden and oogram count was significantly enhanced by both CpE and GSNPs, yet PZQ showed better antiparasitic effects. The antioxidant activity of GSNPs was more efficient, and they significantly restored hepatic (glutathione) as well as reduced (malondialdehyde) and (nitric oxide) levels. In addition, both CpE and GSNPs regulated apoptotic markers by inhibiting Bcl2-cell-associated X protein and enhancing B-cell lymphoma protein 2 expression, thereby inhibiting hepatocyte apoptosis. Histopathological examination revealed a reduction in granuloma size and hepatic fibrosis, along with an improved hepatoprotective potential of GSNPs. Biochemical analysis revealed increased activity of liver enzymes (alanine transaminase, aspartate transaminase, and gamma-glutamyl transferase) as well as markers of renal function (urea and creatinine), indicating they also had a systemic protective role. All treatments resulted in some ultrastructural alterations in worms.

Conclusion: The normalized parasitological and physiological parameters were utilized in developing a novel mathematical framework that facilitates more objective assessments for treatment protocols. Although PZQ showed the highest efficacy against the parasite (total efficacy score: 71.8), the plant extract showed the highest efficacy in anti-fibrotic and anti-apoptotic properties (total efficacy score: 61.6). However, GSNPs showed balanced therapeutic benefits (total efficacy score: 51.1). This study indicated that comparison based on both the host physiological parameters and those of the parasite is more comprehensive for optimal anti-schistosomal treatment selection. This study also confirmed that treatments derived from plant sources may have complementary benefits over traditional chemotherapy through metabolic pathways involved in the host protective responses.

ARTICLE HISTORY

Received 06 August 2025
Revised 28 September 2025
Accepted 01 October 2025
Published 29 December 2025

KEYWORDS

Biogenic nanoparticles; *Schistosoma mansoni*; Sodom apple; Antioxidant enzymes; Apoptotic markers; Liver functions

Introduction

Schistosomiasis affects approximately 600 million people living in tropical and subtropical regions each year, making it the second most common disease in the world after malaria [1]. This situation calls for research into anti-schistosomiasis treatments, especially those derived from plant sources [2]. *Calotropis procera* is a medicinal plant that has been demonstrated to possess anticarcinogenic [3],

Contact Ahmed H. Nigm ahmednigm@sci.asu.edu.eg Department of Zoology, Faculty of Science, Ain Shams University, Cairo, Egypt.

How to cite this article: Hamdan ZK, Namik MF, Mahmood NA, Soliman MI, Abdel-Rasol MA, Nigm AH. Mechanistic insights into *Calotropis procera* extract and green-silver nanoparticles as therapeutic agents in murine schistosomiasis: Targeting *BAX*/Bcl-2 and oxidative stress. J Adv Vet Anim Res 2025; 12(4):1314–1332.

antibacterial [4], anthelmintic [5], and antioxidant [6] properties. In previous studies on schistosomiasis, it was found that the extract of this plant has anti-inflammatory effects in addition to destructive activities on the tegument of worms [5,7].

Metal-fabricated nanoparticles, including those made of silver and gold, have emerged as potential alternatives for treating *Schistosoma* parasites due to their rapid and cost-effective availability [8]. However, their minute size allows them to infiltrate even the body's small blood vessels, concentrating their therapeutic effects on the parasites while minimizing their adverse effects. Additionally, research has shown that silver nanoparticles can effectively combat the *Schistosoma* parasite [9]. Silver nanoparticles were chosen due to their antibacterial effects [10] and high biocompatibility, especially when formed by plant extracts [11]. Additionally, silver nanoparticles are an excellent and inexpensive strategy [12]. The antiparasitic activity of silver nanoparticles is attributed to the release of free silver ions, which affects both the parasite and the host, inducing oxidative stress [8]. Green nanotechnology plays a broader and deeper role, as recent studies have demonstrated its contributions to diverse biomedical and non-biomedical applications [13,14]. Several studies have evaluated the antischistosomiasis effects of *Calotropis*-fabricated silver nanoparticles [10,15].

Calotropis procera (Aiton) W.T. Aiton (family: Apocynaceae) is a perennial shrub widely distributed in desert regions. This plant is rich in bioactive secondary metabolites, including cardenolides, flavonoids, and phenolic compounds, which have demonstrated significant antioxidant, anti-inflammatory, anthelmintic, antibacterial, and anticancer properties [16]. The antischistosomal effect of *Calotropis*-mediated silver nanoparticles was confirmed in a previous study [5]. Therefore, the multifaceted pharmacological profile of *C. procera*, combined with the advantages conferred by plant-mediated nanoparticle fabrication, provides a rational and promising basis for its selection in this comparative investigation.

Most studies focus on the direct effects of treatments on parasite morphology and physiology, neglecting host responses. Yet drug effects in infected mice can differ markedly from those in healthy animals due to parasite-induced changes in the host environment. This necessitates performing simultaneous physiological examinations on the infected murine systems and reducing reliance on data derived from research that applied the same drug on cell lines (*in vitro*) or healthy animals.

In this study, a comparative evaluation of three different treatment protocols against *Schistosoma mansoni* was conducted [intraperitoneal injection with *Calotropis*-mediated silver nanoparticles, oral administration of *Calotropis* extract (CpE), and the praziquantel (PZQ) drug]. This comparison included recording changes in some physiological indicators of the murine system, in addition to the anti-schistosomiasis effects. The applied physiological parameters were the liver enzymes in serum, including aspartate transaminase (AST), alanine transaminase (ALT), and gamma-glutamyl transferase (γ-GT). Besides, apoptotic Bcl2-cell-associated X protein (BAX), and B-cell lymphoma protein 2 (Bcl2), antioxidant (superoxide dismutase (SOD), and catalase (CAT), and hepatic oxidative stress markers [(reduced glutathione (GSH), malondialdehyde (MDA), and nitric oxide (NO)] were measured in liver tissues. The applied parasitological criteria included the recovery of adult worms, oogram pattern, egg count in both the liver and intestine, and the size and number of granulomas, as well as a quick view of the ultrastructural modifications in the adult worm tegument.

Materials and Methods

Ethical approval

All animal procedures and experimental protocols concerning this work were approved by the Ain Shams University Research Ethics Committee (ASU-REC), Egypt (Code: ASU-SCI/ZOOL/2025/3/3).

Chemicals

The plant under investigation was collected from the desert areas in eastern Cairo, specifically near the Joseph Tito Highway, 30°08'20.3"N 31°25'08.7"E. The plant was identified by a colleague (Dr. Mohammed Abdel Fattah) from the Botany Department, and a voucher specimen (giant milkweed-4-17) was deposited at the Department of Botany, Faculty of Science, Ain Shams University (Cairo, Egypt). PZQ (Distocide®) was purchased from EIPICO, El-Asher Men Ramadan (Cairo, Egypt). Cremophore® EL was obtained from Sigma-Aldrich® Chemical Company (Germany).

Preparation of aqueous CpE

The fresh stems of *C. procera* were separated, washed to remove impurities, dried in a shadowed area, and then ground with a mortar apparatus. The distilled water (500 ml) was mixed with the plant powder (300 gm) in a clean glass beaker. The mixture was heated to boiling point (30 min) and then cooled at room temperature. It was subsequently filtered through muslin cloth and Whatman® qualitative filter paper, Grade 1. The filtrate was centrifuged at 2,500 rpm for 15 min to remove any remaining particles, resulting in a clear supernatant that was subsequently stored in a dark container at 4°C for future use.

Preparation and characterization of green silver nanoparticles (GSNPs)

GSNPs were synthesized by adding 15 ml of *C. procera* extract dropwise to a 4 mM silver nitrate solution (0.7 gm $AgNO_3$ in 1 L deionized water), with continuous stirring of the mixture at 60°C–70°C by a thermal magnetic stirrer (FineLab® Scientific, Hong Kong). The color of the mixture changes from pale yellow to dark brown after 4 h, indicating nanoparticle formation. After 24 h, the nanoparticles were collected by centrifugation at 15,000 rpm for 5 min, washed 3 times with deionized water, dried, and stored at 4°C [17]. The structure of GSNPs was confirmed using a UV-vis spectrophotometer (Shimadzu® UV-visible 1,800 Spectrophotometer, Japan). The sample was diluted appropriately to avoid saturation at the plasmon resonance peak. The samples' absorption spectrum was measured between 200 and 1,000 nm with the following settings: double-beam, baseline correction using distilled water, and scan speed of 240 nm/min. To determine the size distribution of the resultant GSNPs, dynamic light scattering (DLS) (Particle Sizing Systems, NICOMP™ 380NLS, Santa Barbara, CA) was employed. Silver nanoparticle suspensions were diluted in ultrapure water to an optimal concentration and filtered to remove dust or large aggregates. Instrumental settings included wavelength 633 nm (He-Ne laser), detection angle: backscatter angles, 3–5 runs of 10–30 sec per run, and 25°C.

The surface adsorption of functional groups on green nanoparticles was studied using Fourier transform infrared (FTIR) spectrum measurements (Jasco® FT/IR 6100, Japan). The sample was deposited as a thin film on a glass substrate, and then the measurements were carried out over the mid-infrared region, typically from 4,000 to 400 cm^{-1} with the following instrumental settings: resolution of 4 cm^{-1}, 32 to 64 scans, atmosphere: nitrogen. Furthermore, the form and particle size of GSNPs were determined with transmission electron microscopy (TEM) on a Philips/FEI Inspect-F (Philips/FEI®, USA). The nanosuspension was diluted appropriately in distilled water, and a drop (5–10 µl) was placed on a carbon-coated copper TEM grid, which was air-dried before imaging. The instrumental settings: 100 to 120 kV, Bright field, thermionic emission gun, and magnification range from 150,000x to 250,000x [18].

Experimental animals and infection

Throughout the study, male Swiss albino mice weighing approximately 20 ± 5 gm at the start of the experiment were employed. The animals were acquired from the Theodor Bilharz Research Institute, Schistosome Biology Supply Centre (SBSC), in Giza, Egypt, and they were kept in appropriate cages for a week to allow them to be acclimatized to the laboratory environment (12-h dark/light cycle with free access to fresh water and a standard commercial pellet diet). The fresh cercariae of *S. mansoni* were also acquired from SBSC for infection. The mice were experimentally infected by fresh *S. mansoni* cercariae (70 ± 10/mouse) via subcutaneous injection [5].

Experimental design

Twenty-five male mice were divided into five groups for this study (n = 5 per group). Group I was the negative control (non-infected), whereas groups II through V were infected with *Schistosoma.* Group II served as the positive control (untreated) group. Group III orally received PZQ, prepared in 2% (v/v) Cremophor EL, at a dose of 500 mg/kg for 2 consecutive days [8,13]. Group IV was orally administered with *C. procera* extract at 200 mg/kg for 15 days [19]. Group V was treated intraperitoneally with a modified dose of GSNPs, 200 mg/kg, administered in six doses over a 2-week period [5]. All treatments were applied in the 6th week post-infection. GSNP suspension was prepared using phosphate buffer vehicles.

Blood sampling and tissue extraction

Animals received isoflurane anesthesia and were sacrificed at the end of the experiment. After the blood samples were collected, they were coagulated in sterile test tubes. The serum was then separated by centrifuging the blood samples at 4,000 rpm for 20 min at 4°C, and subsequently aliquoted and stored at −80°C for further analysis. Immediately after sacrifice, the livers were perfused (Portomesenteric perfusion technique) using cold isotonic citrate saline, which was forced through the hepatic portal vein to collect all recovered worms from the hepatic and Portomesenteric veins. The livers were then dissected, weighed, and kept in aluminum foil at −80°C. For further preparation, liver tissues were washed with cold isotonic saline, and 1 gm of liver was homogenized in 10 ml of cold 0.1 M potassium phosphate buffer (pH 7.3). The homogenate was centrifuged at 10,000 rpm for 20 min at 4°C; the supernatant was collected and stored at −80°C for subsequent assays, with an aliquot retained for protein determination.

Parasitological parameters

Total worm burden (TWB)

After 2 weeks of treatment, mature schistosomes were recovered from the portal mesenteric veins according to the protocol [20].

Oogram count

The proportions of various egg developmental stages (immature, mature, or dead) in the intestines were examined as described in [21]. The number of eggs at each stage

was divided by the overall egg count corresponding to a given weight of intestinal tissue.

Tissue egg loads of the hepatic/intestinal tissues

The liver and intestines were sampled (two samples per organ), weighed, and then frozen at −20°C. A potassium hydroxide (KOH) solution (4%) was used to digest the samples. The total number of eggs in the liver and intestines was calculated according to [22]. Briefly, the tissue egg load was calculated as follows: the mean of the egg number in homogenized tissue = the mean number of eggs in the microscopically examined sample was multiplied by the volume of digested tissue, and then it was divided by the volume of the microscopically examined sample. Then, the mean number of ova per gram in the infected organ was computed as the sum of the number of ova/gm in two representative samples and dividing the result by 2.

Histopathological studies

The isolated pieces of liver were rinsed in 10% formal saline and subsequently fixed in a 10% neutral buffered formalin solution. For sectioning, the specimens were rinsed with distilled water, dehydrated, and embedded in paraffin wax. Five sections (5-µm thickness) were placed on a clean glass slide for each liver sample. The transparencies were deparaffinized and stained with trichrome, hematoxylin, and eosin stains. The hepatic lesion containing a central single ovum was employed to achieve microscopical examination of specimens [23]. Furthermore, the mean diameter of the selected granuloma was determined by obtaining the maximal diameter and its perpendicular one [24].

Transmission electron microscopy

The recovered worms were washed with physiological saline and then fixed for 2 h in 3% glutaraldehyde and 0.1 M phosphate buffer (PH 7.4). Then, the specimens were subjected to post-fixation in 1% osmium tetroxide for 1 h, followed by dehydration and embedding in epoxy resin. The semithin sections were stained with methylene blue and examined by light microscope (Olympus® CX23 binocular microscope, Japan), and then the ultrathin sections were stained with uranyl acetate/lead citrate and examined by TEM (Philips/FEI Inspect-F, Philips/FEI®, USA) in the regional center for mycology and biotechnology, Al-Azhar University, Cairo, Egypt.

Biochemical assays

Oxidative stress and antioxidant markers were assessed in liver tissue homogenates. The parameters investigated included MDA, NO, SOD, CAT, and reduced GSH. The activities of these markers were determined according to [25–29], respectively. Additionally, the apoptotic markers (*BAX* and Bcl-2) were measured in the homogenates of liver using ELISA kits: *BAX* (Catalog No: SEB631R, Cloud-Clone® Corp., USA) and Bcl-2 (Catalog No: E-EL-R0648, Elabscience® Biotechnology Inc, USA), following the manufacturer's instructions. The liver enzymes (AST, ALT, and γ-GT) as well as kidney function indicators (urea and creatinine), were also analyzed.

Statistical analysis

The data were given as mean ± standard error of the mean (SEM). To evaluate statistically significant differences among experimental groups, One-way analysis of variance (ANOVA) was implemented, followed by Tukey's multiple comparison test. *P*-values were considered significant when $p < 0.05$. SPSS software, version 24, was used for data analysis, Chicago, IL.

Results

Characterization of GSNPs

UV-visible spectroscopy was employed to verify the formation of green nanoparticles. The maximum spectral absorption was observed at 426 nm, which is indicative of silver nanoparticles (Fig. 1A). In contrast, the particle size analysis conducted using DLS demonstrated the formation of a polydisperse population of nanoparticles within a 110 nm range (Fig. 1B). The transmission microscopical examination showed that synthesized GSNPs have a relatively uniform spherical pattern with an average diameter of 108.5 ± 32 nm (Fig. 1C). The infrared spectra (FTIR) of both the plant extract (CpE) and GSNPs showed that the bands of the absorption of both the extract and GSNPs were more or less identical; that means the presence of capping agents over the surfaces of the formed silver nanoparticles (Fig. 1D, E).

Parasitological parameters

The TWB

It was observed that none of the treated groups recovered any female worms, which represented a statistically significant difference ($p < 0.05$) from the infected control group. The most significant reduction in worm burden was observed in the PZQ-treated group (90.6%), with statistical differences ($p < 0.05$), followed by the plant extract-treated group (60.47%) (Table 1).

The oogram pattern

The PZQ-treated group exhibited the greatest percentage of dead eggs (94%, *p*-value < 0.05). Furthermore, the percentage of dead embryos in both groups treated with either plant extract or green nanoparticles is not significantly different (16.4%and 11.8%, respectively). Conversely, the PZQ-treated group did not exhibit any immature eggs (Table 2).

Tissue egg load

In comparison to the infected group, the PZQ-treated group exhibited the maximum reduction percentage of total egg count in tissue (92.7%), followed by the plant extract-treated group (29.39%) (Table 3). It was observed that the number of ova in the liver was significantly lower in the CpE group than in the intestine. Conversely, the GSNPs or CpE-treated groups did not exhibit significant reductions in tissue egg load of the intestine.

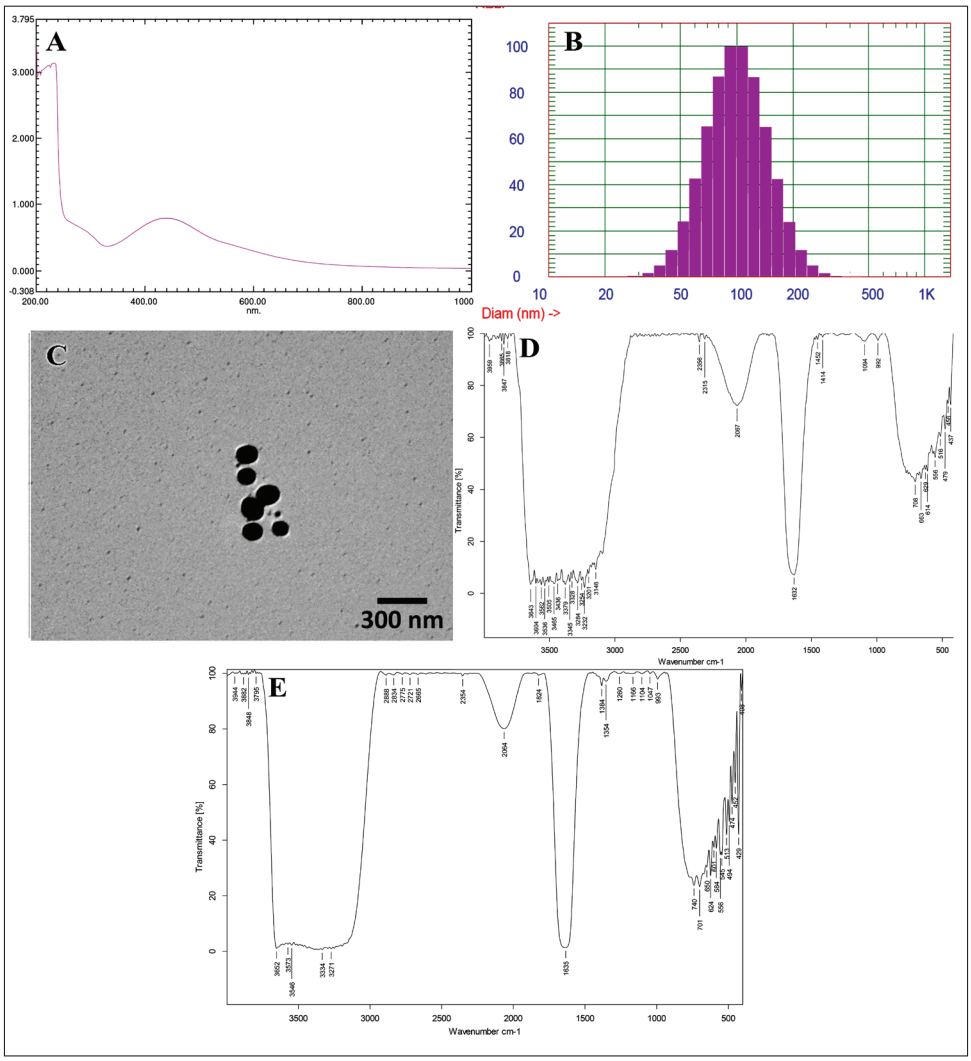

Figure 1. Characterization of GSNPs. A: UV-vis spectra, B: DSL analysis, C: TEM profiles, D: FTIR spectra of plant extract, E: FTIR spectra of GSNPs.

Table 1. The impact of treatments on the mean worm burden of various groups in comparison to the infected control group.

Groups	Male	Female	Couples	Total	Worm burden reduction (%)
Infected	1.8 ± 0.2	0.8 ± 0.20	3.4 ± 0.50	8.6 ± 1.07	------
Infected + PZQ	0.00[a]	0[a]	0.4 ± 0.5[a]	0.8 ± 1.0[a]	90.6
Infected + CpE	0.6 ± 0.4[a]	0[a]	1.4 ± 0.24[a]	3.4 ± 0.4[a]	60.47
Infected + GSNPs	1.2 ± 0.2[b]	0[a]	1.6 ± 0.24[a]	5.0 ± 0.63[ab]	48.8

Results are expressed as the Mean ± SEM. [a, b] indicate significant differences versus infected and PZQ groups, respectively at *p*-value < 0.05.

Histopathological changes in liver tissues

The negative group showed normal liver architecture (Fig. 2A), including the reticular architecture of hepatocytes (Fig. 2B), healthy portal zones (Fig. 2C), and normal central veins (Fig. 2D), with no inflammatory infiltration observed. In the infected group, schistosomiasis-related histopathological aspects were observed, including numerous scattered fibrocellular granulomas (Fig. 2E), particularly in the subcapsular hepatic regions (Fig. 2F), with inflammatory infiltrates surrounding the dilated portal spaces (Fig. 2G). In addition, inflammatory infiltrations were observed around the slightly dilated central vein (Zone III) (Fig. 2H).

In comparison to the infected group, the PZQ-treated group exhibited the maximum reduction in granuloma size and count (46.3% and 74.8%, respectively) (Table 4; Fig. 2I, G). Lower reductions in the granuloma size/count (19.3%, 28%, respectively) were observed in the CpE-treated group (Fig. 2M, N).

On the other hand, the GSNPs-treated group exhibited only a significant change in granuloma count (16%) (Fig. 2Q, R). Concerning the histopathological changes, the GSNPs-treated group showed a better healthy profile in the portal spaces and centrilobular zone (Fig. 2S, W). In contrast, the PZQ and, to a lesser extent, CpE-treated groups exhibited inflammatory infiltrates in these areas, along with dilatations in both portal and central veins (Fig. 2K, L, O, P).

Table 2. Oogram patterns in various treated groups versus the infected control one.

Groups	Immature ova	Mature ova	Dead ova
Infected	50.4 ± 0.50	44.8 ± 0.96	5.0 ± 0.31
Infected + PZQ	0 ± 0[a]	6.0 ± 0.44[a]	94.0 ± 0.44[a]
Infected + CpE	42.2 ± 1.49[ab]	41.4 ± 0.60[b]	16.4 ± 1.12[ab]
Infected + GSNPs	42.8 ± 1.15[ab]	45.4 ± 2.08[b]	11.8 ± 1.39[abc]

Results are expressed as the Mean ± SEM. [a, b, c] indicate significant differences versus infected, PZQ, and CpE groups, respectively at *p*-value < 0.05.

In the infected group, most of the granulomas were fibrocellular (Table 4), composed of inner thick fibrous layers and outermost layers of inflammatory cells (Fig. 3). The percentage of fibrocellular granulomas was greatly increased in the PZQ-treated group (96.3%), followed by that of the plant extract-treated one (90.6%) (Table 4). It was noticed that the fibrous content of the granuloma (in hepatic sections stained with trichrome) was generally the lowest in plant extract-treated mice (Fig. 3).

TEM examination of recovered adult worms

The potential surface modifications in the tegument of male worms were briefly examined in this study. In the untreated infected group, the male tegument was highly convoluted, with numerous large channels that were open on the surface; moreover, tubular invaginations formed from the basal lamina into the tegument. The musculature was continuous with the normal healthy architecture and prominent spiny tubercles (Fig. 4A, B). In the extract-treated group, a highly folded tegumental surface (in the dorsal side of the worm) was observed with the presence of an obvious collapse in tubercles and discontinuity during the subtegumental musculature (Fig. 4C). Besides, the tegument showed some blebs around tubercles accompanied by dead parenchymal cells (Fig. 4D). Characteristic abnormal aggregations of mitochondria were observed, especially in tegumental regions under spines with large vacuoles in parenchyma (Fig. 4E, F). In the GSNP-treated group, the tegument exhibited a minimum state of pathological changes where the normal-sized tubercles had blunted, short, reduced spines (Fig. 4G); the remaining ultrastructural features of the tegument were normal (Fig. 4H).

Biochemical analysis

The infection with *S. mansoni* led to a notable decrease in hepatic reduced GSH levels, showing a reduction of 21.27% when compared to the uninfected group (Fig. 5A). The administration of PZQ, CpE, and GSNPs led to a significant restoration of hepatic GSH levels, achieving increases

Table 3. The mean number of ova per gm of liver and intestinal tissues in different treated groups versus infected control one.

Groups	Ova counts in liver (ova/mg tissue)	Ova counts in intestine (ova/mg tissue)	Total ova/mice	Reduction on ova count (%)
Infected	3,009.8 ± 320.31	2,916.4 ± 258.93	5,926.2 ± 471.76	-----
Infected + PZQ	227.2 ± 12.75[a]	203.8 ± 22.49[a]	431 ± 30.69[a]	92.73
Infected + CpE	1,917.4 ± 327.27[ab]	2,267.2 ± 63.22 [b]	4,184.6 ± 366.27[ab]	29.39
Infected + GSNPs	2,249.2 ± 43.97[ab]	2,548.2 ± 355.26 [b]	4,797.4 ± 334.62[b]	19.05

Results are expressed as the Mean ± SEM. [a, b] indicate significant differences versus infected and PZQ groups, respectively at *p*-value < 0.05.

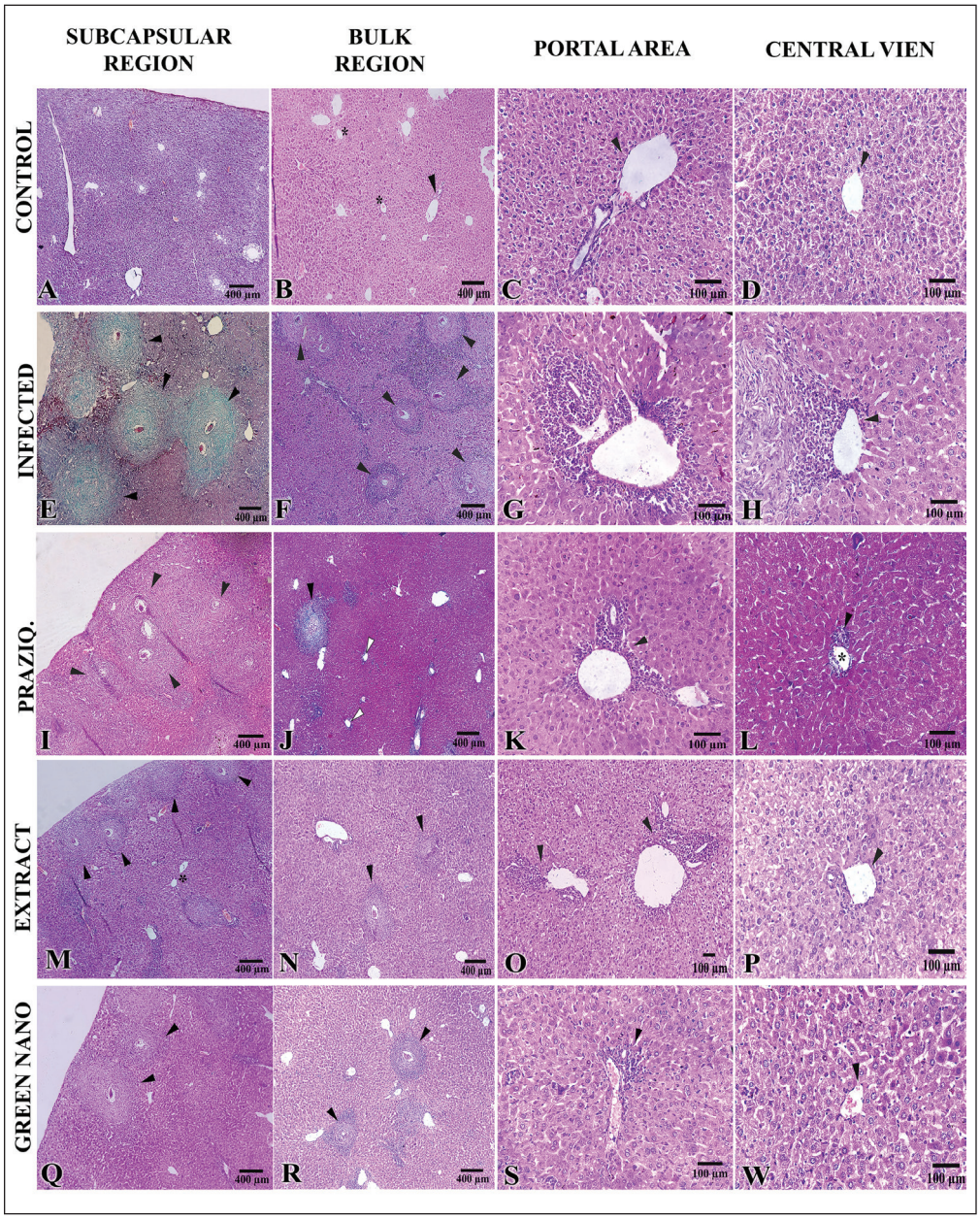

Figure 2. Sections of the liver show the histological features in the experimental groups. A–D: negative control group. E–H: The infected group. I–L: PZQ-treated group. M–P: Plant extract group. Q–W: GSNPs-treated group.

of 19.19%, 34.33%, and 51.33%, respectively, when compared to the untreated infected group. The infection with *S. mansoni* resulted in a significant elevation of hepatic MDA and NO levels, with increases of 98.7% and 419.4%, respectively, compared to the uninfected group (Fig. 5B, C). The application of PZQ, CpE, and GSNP led to a notable decrease in oxidative stress markers. PZQ led to a reduction in hepatic MDA and NO by 39.33% and 52%, respectively, while CpE showed reductions of 50.98% and 72.8%, and GSNPs resulted in decreases of 58.66% and 66.4% when compared to the untreated infected group. Generally, it was found that the orally plant extract-treated group showed an antioxidant profile closer to that of the uninfected group (Fig. 5D).

In terms of apoptotic markers, a significant rise in hepatic *BAX* concentration (44.4%) was observed in *S. mansoni*-infected mice when compared to the non-infected control group (Fig. 6A). Nonetheless, administration of

Table 4. The mean of numbers and sizes of hepatic granulomas in treated groups versus infected one.

Animal groups	Granuloma diameter (mean ± SE)	% Reduction in granuloma size	No of granuloma (mean ± SE)	% reduction (mean ± SE)	Types of granulomas			State of S. mansoni eggs	
					Cellular %	Fibro/ cellular%	Fibrous%	Intact	Degenerated
Infected	315.49 ± 15.73	------	10.6 ± 0.57	------	26 ± 3.61	74 ± 3.61	0	92 ± 1	8 ± 1
Infected + PZQ	169.18 ± 13.48[a]	46.3	2.67 ± 0.47[a]	74.8	1.67 ± 1.53[a]	96.33 ± 4.04[a]	0	17.33 ± 2.5[a]	82.67 ± 2.52[a]
Infected + CpE	254.04 ± 21.44[ab]	19.3	7.64 ± 0.86[ab]	28	21.33 ± 4.04 b	86 ± 6.56	0	55 ± 3[ab]	45 ± 3[a]
Infected + GSNPs	312.32 ± 5.17[b]	1	8.8 ± 0.62[b]	16	25.67 ± 4.04[b]	74.33 ± 4.04	0	90 ± 1[bc]	10 ± 1

Results are expressed as the Mean ± SEM. [a, b, c] indicate significant differences vs. infected, PZQ, and CpE groups, respectively at p-value < 0.05.

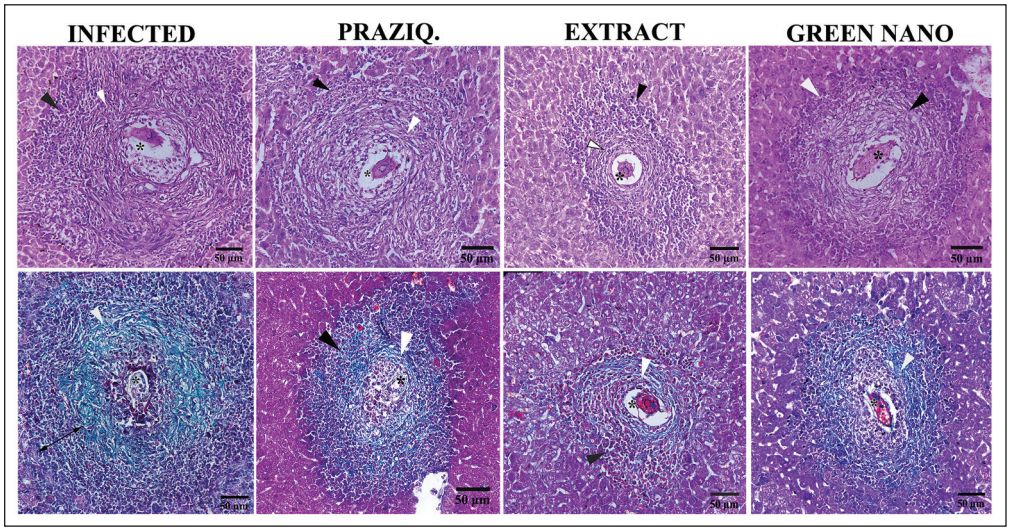

Figure 3. High-power magnifications for granulomas showing the size and the histological features of granulomas, the upper row for sections stained with H&E, and the lower one stained with trichrome stain (white arrowheads represent the fibrous layers, black arrowheads represent inflammatory cells, and asterisks represent the ova).

PZQ, CpE, and GSNP resulted in significant decreases in hepatic *BAX* levels, with reductions of 21.4%, 48.9%, and 34.6%, respectively, when compared to the untreated infected group. Furthermore, the apoptotic pattern of the GSNP-treated group was found to be more similar to that of the uninfected group. The infected untreated group showed a decrease in the hepatic Bcl-2 concentration (31.1%) in relation to the uninfected group (Fig. 6B). PZQ, CpE, and GSNP treatments demonstrated a remarkable recovery in the Bcl-2 levels (32%, 25.7%, and 24.9%, respectively) compared to the untreated infected group. The *BAX*/Bcl-2 ratio was more or less similar in the negative control (0.277) as compared to the CpE- and GSNP-treated groups (0.236 and 0.304). The PZQ group revealed a higher ratio (0.347). This study suggests that the plant extract has therapeutic potential in promoting recovery from apoptosis.

Infection with *S. mansoni* resulted in substantial increases in serum ALT, AST, and γ-GT activity, with elevations of 368.35%, 409.33%, and 767.50%, respectively, in comparison to the uninfected group (Fig. 7A–C). Pharmacological intervention with PZQ, CpE, or GSNPs substantially reduced these elevations. PZQ specifically diminished serum ALT, AST, and γ-GT activity by 64.05%, 63.87%, and 65.18%, respectively. CpE diminished these enzyme activities by 52.16%, 55.45%, and 61.09%, whereas GSNP therapy decreased them by 28.38%, 34.30%, and 36.34%, respectively, compared to the untreated infected group. The PZQ-treated group had liver function profiles similar to those of the uninfected control group, followed by the CpE-treated group (Fig. 7D).

Infection with *S. mansoni* markedly reduced hepatic SOD and CAT activity by 52.28% and 40%, respectively, in comparison to the untreated group (Fig. 8A, B). The

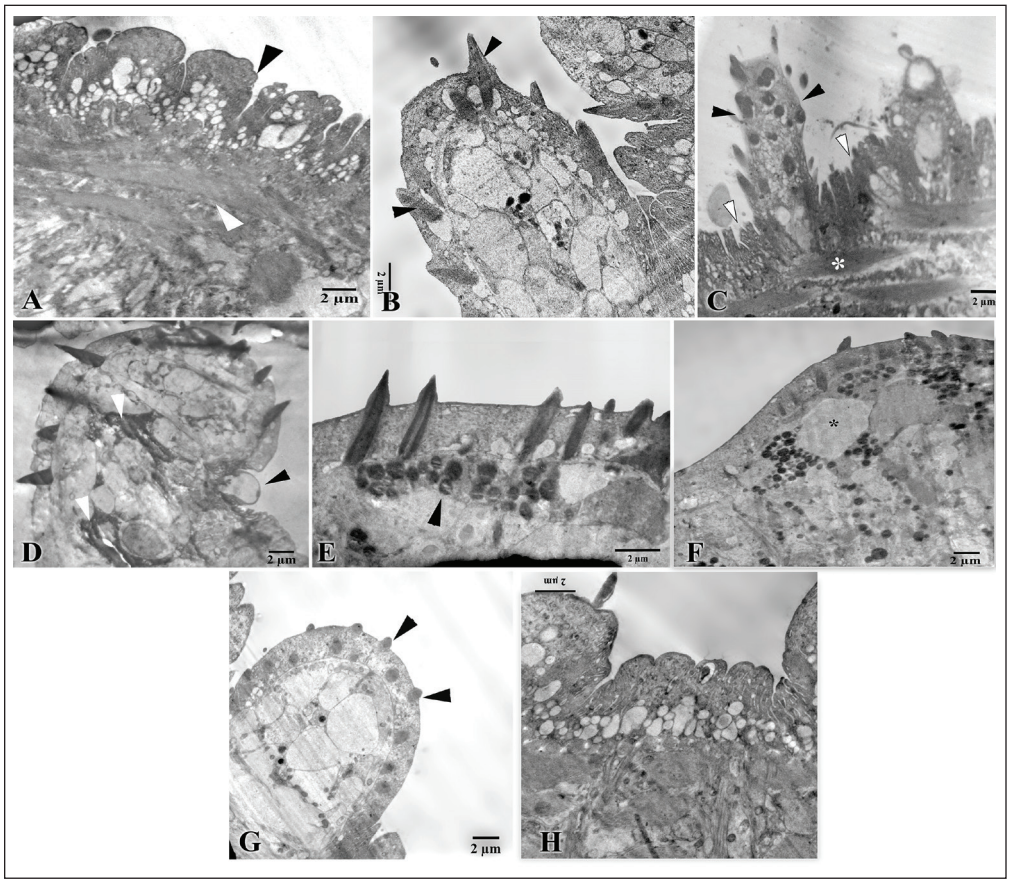

Figure 4. TEM of the tegumental surface of an *S. mansoni* male. A–B: Control group; A, the tegument shows a healthy appearance, including the highly convoluted outer surface (black arrowhead) and the prominent musculature (white arrowhead). B, a tubercle with prominent sharp spines (black arrowheads). C–F: Extract-treated group; C, the tegumental surface is highly folded (white arrowheads) with the presence of an obvious collapse in tubercles (black arrowheads). D, the tegument shows a bleb in the base of a tubercle (black arrowhead), besides some dead parenchymal cells (white arrowheads). E, Abnormal aggregations of mitochondria in a parenchymal region under the tegument, which contains spines (black arrowhead). F, large vacuoles in the parenchymal region (asterisk). G–H: G, Green nanoparticle-treated group: the normal-sized tubercles with blunt, short, reduced spines (black arrowheads). H, The tegumental area with a normal profile.

administration of PZQ resulted in a moderate 17.9% enhancement in CAT activity. Conversely, treatment with CpE and GSNPs led to significant enhancements in both CAT and SOD activity. CpE enhanced CAT and SOD activities by 51.3% and 70.42%, respectively, whereas GSNPs augmented these activities by 56.6% and 68.24% compared to the untreated infected group.

Serum urea and creatinine levels were significantly increased by *S. mansoni* infection, showing increases of 101.79% and 153.73%, respectively, compared to the uninfected group (Fig. 9A, B). The administration of PZQ, CpE, and GSNPs markedly diminished these increases. CpE diminished urea by 30.09% and creatinine by 41.18%, while PZQ lowered urea and creatinine levels to their minimum values of 42.05% and 42.35%, respectively. The GSNP treatment resulted in reductions in urea and creatinine levels, which decreased by 15.04% and 13.53%, respectively, compared to the untreated group. The PZQ-treated group demonstrated a kidney function profile similar to that of the uninfected group, followed by the CpE-treated group. All tables related to the above-mentioned data graphs of biochemical analysis are in Supplementary Tables 1–5.

To objectively evaluate the three existing protocols for treating schistosomiasis, physiological criteria of the infected host must be considered in conjunction with parasitological criteria. To achieve this evaluation, two methods may be employed: either a visual evaluation using a heat map or a numerical evaluation using statistical methods. First, all criteria, whether parasitic or physiological, must first be measurable accurately. Physiological criteria

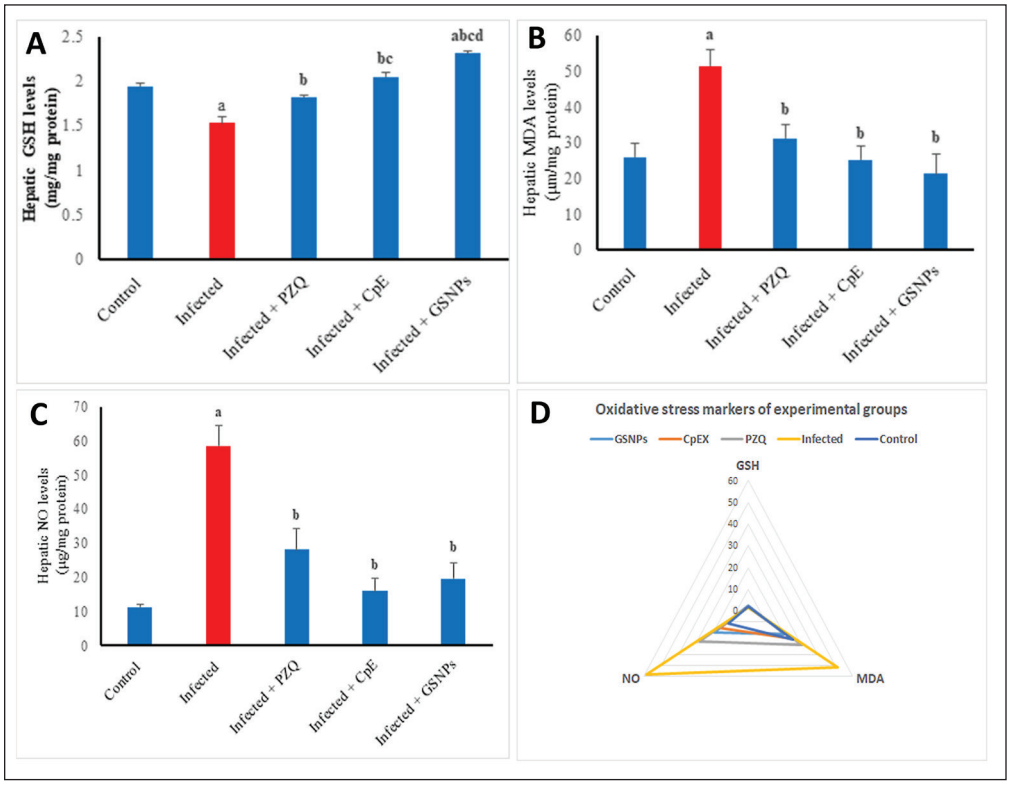

Figure 5. A–C: Effect of CpE, GSNPs, and PZQ on hepatic oxidative stress markers. A) Reduced GSH, B) MDA, C) NO, D) Antioxidant profile of experimental groups. Results are expressed as the Mean ± SEM. [a, b, c, d] are significant differences vs. the control, infected, PZQ, CpE, and GSNPs groups, respectively, at a *p*-value < 0.05.

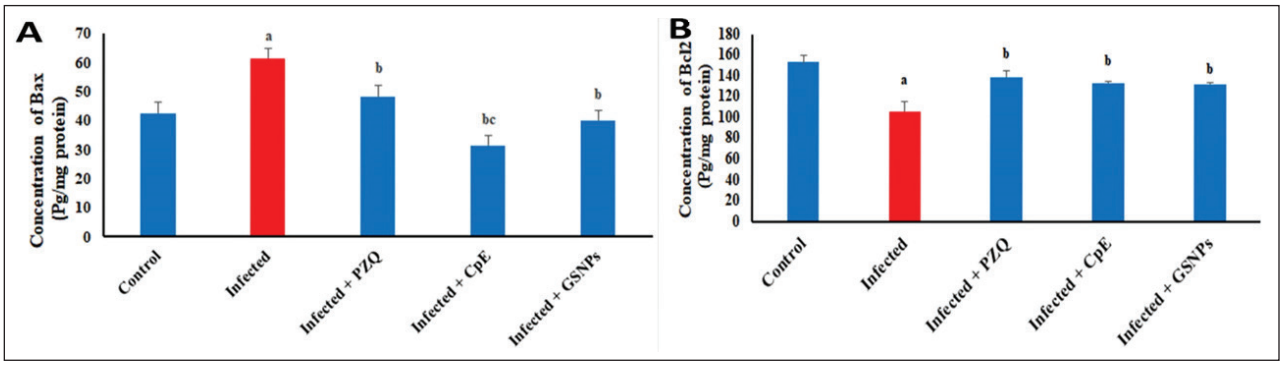

Figure 6. Effect of CpE, GSNPs, and PZQ on hepatic protein concentration of A) *Bax* and B) Bcl-2. Results are expressed as the Mean ± SEM. [a, b, c, d] are significant differences versus the control, infected, PZQ, CpE, and GSNPs groups, respectively, at a *p*-value < 0.05.

should be assessed in non-infected animals to establish standard values, which serve as a basis for calculating normalization percentages (or recovery ratios) in comparison to analogous physiological criteria in infected animals. This study established normalization percentages for the physiological criteria of infected mice (GSH, MDA, NO, *BAX*/Bcl-2, ALT, AST, γ-GT, SOD, CAT, urea, and creatinine) and those related to the parasite (*Schistosoma*), including reductions in worm burden, tissue egg load, granuloma number, granuloma size, and percentage of dead eggs, within each treatment protocol separately, as presented in Table 5. All normalization percentages of this study were represented in the visual graph "heat mapping" (Fig. 10), which shows that PZQ treatment is superior to other protocols.

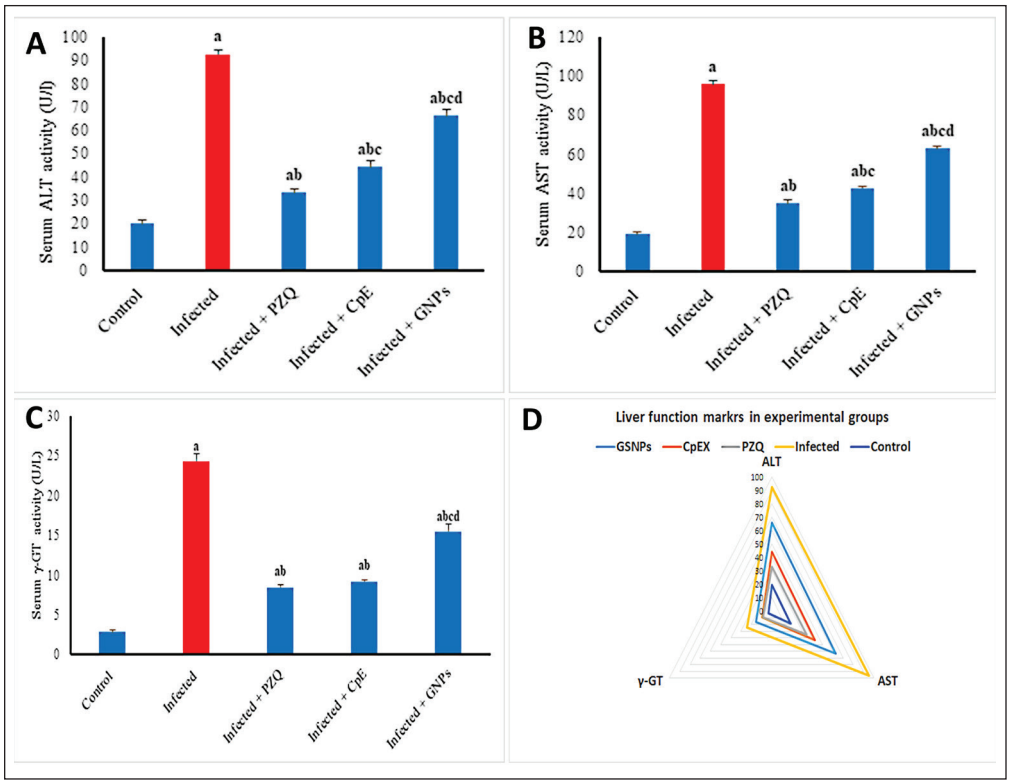

Figure 7. A–C Effect of CpE, GSNPs, and PZQ on serum A) ALT, B) AST, C) *γ*-GT. D General profile of liver function markers in experimental groups. Results are expressed as the Mean ± SEM. [a, b, c, d] are significant differences versus the control, infected, PZQ, CpE, and GSNP groups, respectively, at a *p*-value < 0.05.

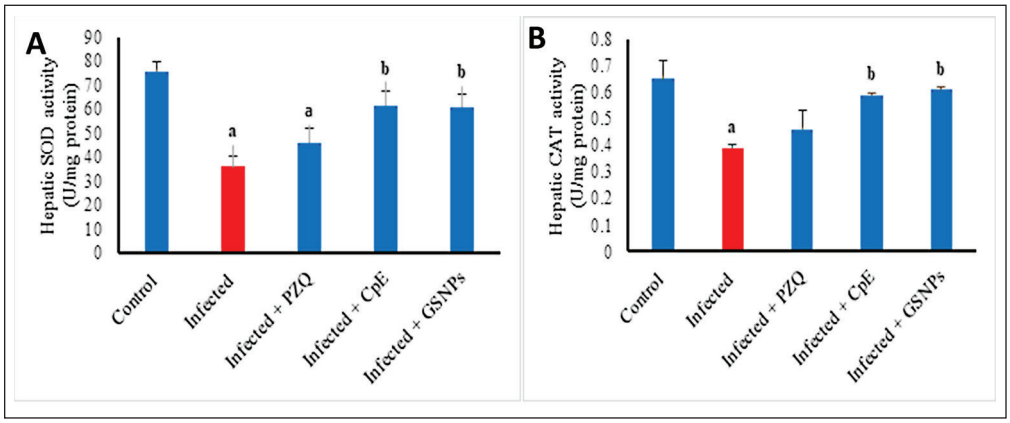

Figure 8. Effect of CpE, GSNPs, and PZQ on hepatic antioxidant enzyme activities. A) SOD and B) CAT. Results are expressed as the Mean ± SEM. [a] indicates a significant difference versus control, and [b]indicates a significant difference versus the infected group at a *p*-value < 0.05.

Regarding numerical evaluation, it was found that using the simple averaging statistical method [Arithmetic Mean (Equal Weight)] for all the present normalization percentages may be inaccurate because it mixes parasitological and physiological criteria, which are relatively independent, potentially masking strengths or weaknesses in each area. To address this, we calculated two separate efficacy scores (arithmetic mean of normalization percentage) for each protocol: one for parasitological criteria and one for physiological criteria. The equations used were as follows:

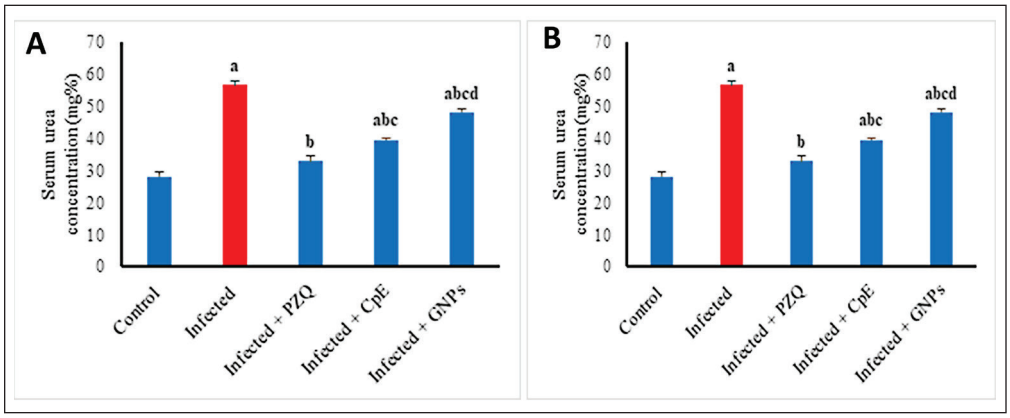

Figure 9. Effect of CpE, GSNPs, and PZQ on concentration of serum A) Urea and B) Creatinine. Results are expressed as the Mean ± SEM. [a, b, c, d]are significant differences versus the control, infected, PZQ, CpE, and GSNP groups, respectively, at a *p*-value < 0.05.

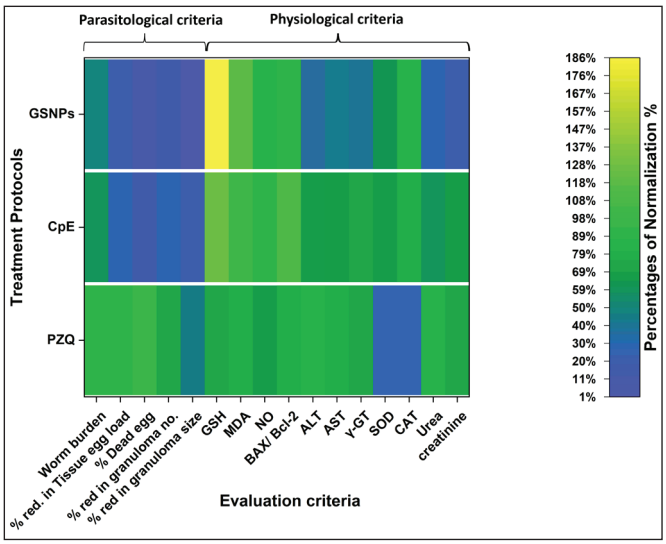

Figure 10. A heat map shows the normalization percentages in three therapeutic protocols applied in the Schistosomiasis-infected murine system.

$$\text{Parasitological efficacy of protocol } (PEP) = 1/n_P \sum_{j=1}^{n_p} xP_i$$

where n_f = number of parasitological criteria and x_{fi} = normalization percentage for parasitological criteria.

$$\text{Physiological Efficacy of protocol } (PhEP): \ 1/n_f \sum_{i=1}^{n_f} x_{fi}$$

where n_f = number of physiological criteria and x_{fi} = normalization percentage for physiological criteria.

A single numerical outcome for protocol evaluation can be created using a mathematical equation that combines parasitological and physiological efficacy scores. This technique can be customized based on biological priorities or statistical logic. The "Weighted Mean" is a statistical method that provides a comprehensive numerical value that reflects the overall effectiveness of the protocol across both measured *PEP* and *PhEP* criteria. It facilitates objective comparison between protocols, even if their effects on individual parameters or criteria differ. "Weighted Mean" method depends on assigning weights to the values for which the mean is to be calculated.

In the present study, there are two sets of criteria (parasitic and physiological) with two calculated values (*PEP* and *PhEP*) for each protocol (Table 6); to calculate the Weighted Mean of normalization percentage for each protocol [Total Efficacy of Protocol (TEP)], the weights should be distributed according to the practical importance of each set. The present physiological criteria were identified as clinically important and deserved 0.60 of the total weight, and the parasitological criteria were 0.40. TEP was calculated as follows:

TEP = PEP × its weight (0.4) + $PhEP$ × its weight (0.6)

PEP = Arithmetic Mean of normalization percentage for a set of parasitological criteria

$PhEP$ = Arithmetic Mean of normalization percentage for a set of physiological criteria

According to this statistical method and Tables 5 and 6, the Total Efficacies of the Protocols were 71.8%, 61.6%, and 51.1% for PZQ, CpE, and GSNPS, respectively (Table 6). Hence, this method considers the overall evaluation, not just the experiment's results but also the weight and importance of each measurement group in relation to the research objective. It was found that the effectiveness of the herbal treatment protocol was very close (despite its poor parasitic results) to that of PZQ. This is due to the herbal anti-apoptotic properties and its reducing effect on oxidative stress.

Table 5. Normalization percentages of various experimental criteria of the whole study for evaluation of the total efficacies of the three treatment protocols.

	Parasitological criteria					The physiological criteria of the host								
Protocol	**% red. Worm burden**	**% red. Tissue egg load**	**% Dead egg**	**% red. granu. no.**	**% red. granu. size**	**GSH**	**MDA**	**NO**	**BAX/ Bcl-2**	**ALT**	**AST**	**γ-GT**	**SOD**	**CAT**	**Urea**	**creatinine**
PZQ	90.60%	92.70%	94%	74.80%	46.30%	71.40%	79.20%	64.40%	80%	81.40%	79.40%	73.60%	24.60%	25.40%	83.30%	69.40%
CpE	60.40%	29.30%	16.40%	28%	19.30%	125.60%	102.30%	90%	112%	66.30%	69%	70.10%	64.30%	77.40%	59.60%	67.90%
GSNPs	48.80%	19%	11.80%	16%	1%	186%	118%	82.20%	93%	36%	42.60%	41%	62.30%	82.60%	29.80%	21.80%
	Parasitological criteria					The physiological criteria of the host										
Protocol	% red. Worm burden	% red. Tissue egg load	% Dead egg	% red. granu. no.	% red. granu. size	GSH	MDA	NO	BAX/ Bcl-2	ALT	AST	γ-GT	SOD	CAT	Urea	creatinine
PZQ	90.60%	92.70%	94%	74.80%	46.30%	71.40%	79.20%	64.40%	80%	81.40%	79.40%	73.60%	24.60%	25.40%	83.30%	69.40%
CpE	60.40%	29.30%	16.40%	28%	19.30%	125.60%	102.30%	90%	112%	66.30%	69%	70.10%	64.30%	77.40%	59.60%	67.90%
GSNPs	48.80%	19%	11.80%	16%	1%	186%	118%	82.20%	93%	36%	42.60%	41%	62.30%	82.60%	29.80%	21.80%

Table 6. Total efficacies of three treatment protocols according to "Weighted Mean".

Protocol	*PEP* %	*PhEP* %	*TEP* = *PEP* * (0.4) + *PhEP* * (0.6)
PZQ	79.68	66.55	31.872+39.93 = 71.8
CpE	30.68	82.23	12.27+49.33 = 61.6
GSNPs	19.32	72.30	7.72+43.38 = 51.1

Discussion

This study aims to conduct a comprehensive objective evaluation of the use of three anti-schistosomiasis treatment protocols: natural extract (*C. procera*), nanomaterial (GSNPs), and reference drug (PZQ). This evaluation is based not only on the anti-schistosomiasis effects, as is usual in most studies, but also includes the physiological responses of the host, especially the liver profile.

The extract of *C. procera* exhibited significant anti-schistosomal activity, primarily through its effects on *S. mansoni*. Research indicates that both alcoholic and aqueous extracts of this plant can reduce recovered worm and tissue egg load in infected mice, demonstrating its potential as a therapeutic agent against this neglected disease [7,30]. Likewise, biogenic silver nanoparticles showed similar pharmacological effects against schistosomiasis. According to antiparasitic efficacy, it was found that the present therapeutic effect of the plant extract was stronger (in view of the worm burden, the egg tissue load, the oogram pattern, and the hepatic granuloma analysis) than that of the green nano-silver, in contrast to some other studies that showed that the effect of the green nano-silver was as close as to the strong effect of PZQ [5]. This difference can be explained by the fact that the present plant extract was given for a longer period of up to 15 days, so the outcomes of some parasitic parameters (worm burden and the size reductions of granulomas) were higher than those of a previous study [7], which applied *Calotropis* administration for only 5 days (60.4% and 19.3% *vs.* 46.4% and 11.22%, respectively). In addition, the larger size of the present GSNPs, reaching 108 ± 32 nm compared to 70–90 nm in Hamdan's study, causes a decrease in the therapeutic effect of the nanoparticles. It is worth noting that the present size variation among DLS and TEM data can be attributed to the fact that DLS measures the hydrodynamic diameter of particles in the solution, which includes the solvation shell and the green capping agents, while TEM measures the actual physical dimensions of dried particles under vacuum conditions [31]. The lack of accurate nanoparticle dose measurement using sophisticated analytical methods, such as inductively coupled plasma or graphite furnace atomic absorption spectrometry, is acknowledged as a drawback of our investigation. This restriction resulted from the limited availability of such equipment throughout the study period.

Regarding the tegumental modifications induced by the three treatments, it is known that these ultrastructural changes, resulting from the action of therapeutic agents, are one of the tools for diagnosing their therapeutic efficacy. Few studies have been conducted on the effect of silver nanoparticles and CpE on the tegument of adult worms [5]. These tegumental changes included atrophy or collapse of the tubercles, sloughing, shortening of spines, and the formation of blebs. In the present TEM, similar variable alterations were observed in the worm tegument treated with either the silver nanoparticles or the plant extract. The plant extract-treated tegument showed an accumulation of mitochondria under the tegument in places where spicules were present. This finding may indicate the pharmacological effect of the extract compounds on the tegumental areas in the spicule region, which may increase oxidative stress in these areas [32].

PZQ treatment produced the greatest reduction in both granuloma size and number, while *C. procera* extract showed moderate effects, and GSNPs had a limited but notable impact. However, CpE-treated mice exhibited the lowest fibrous content in granulomas, indicating a potential role in reducing fibrosis progression (antifibrotic effect), which is regarded as a significant finding for promoting a healthy liver profile [33]. The anti-fibrotic properties of the plant extract can be explained by considering several possible mechanisms. First, it significantly increases the activity of antioxidant enzymes (SOD and CAT), resulting in a reduction in the levels of oxidative stress markers (MDA and NO), as reported in the present study. This antioxidant effect helps neutralize both reactive oxygen species (ROS) and nitrogen species, which are involved in the activation of hepatic stellate cells (HSCs) and the progression of hepatic fibrosis. Thus, the liver cells are protected from oxidative damage. Second, the extract's phytochemicals, including triterpenes such as Pomolic acid, inhibit the viability and activation of HSCs, the key cells responsible for extracellular matrix and collagen synthesis in fibrosis [34]. Third, CpE reduces pro-inflammatory cytokines (e.g., interleukin-8) and, consequently, the inflammatory cell infiltration. The anti-inflammatory action helps decrease inflammatory stimuli that promote fibrosis through immune cell activation and HSC stimulation [35]. This was evident in the present histological sections of the liver in the extract-treated group, which showed a lack of immune infiltration around the central veins and portal areas, especially when compared to those in the PZQ-treated group. Fourth, extract administration increased serum albumin levels, indicating improved liver synthetic function and hepatocyte regeneration [33]. Albumin acts as an anti-inflammatory mediator by inhibiting TNF -α expression and NF-κB activation, thereby contributing to the resolution of fibrosis [36].

Likewise, GSNPs have shown a similar efficacy to that of the plant extract, considering the antifibrotic effect through the same possible mechanisms mentioned earlier. The studies demonstrated that silver nanoparticles inhibited the activation of HSCs and induced their apoptosis in a size- and dose-dependent manner [37]. Furthermore, the biosynthesized silver nanoparticles also downregulate matrix metalloproteinases (MMP-2 and MMP-9), which play a role in tissue remodeling during fibrosis [38,39]. Besides, GSNPs significantly support antioxidant defenses by scavenging ROS [40,41].

Regarding the liver enzymes, schistosomiasis resulted in the elevation of liver enzymes, including ALT, AST, and γ-GT. Increased activity of ALT indicates liver injury, while increased activity of AST points to injury in peripheral tissues. γ-GT is the most markedly increased enzyme, and because γ-GT is associated with bile duct enzymes, this indicates a bile obstruction most likely due to a granuloma, which causes fibrosis and liver function impairment [42]. Considering the treatment protocols in this study, it was found that the liver enzymes (ALT, AST, and γ-GT) were most improved after PZQ, followed by plant extracts, and although PZQ was not superior in increasing the antioxidant activity, it has this superiority in the normalization of liver enzymes [43,44]. Several reported studies indicate that liver enzymes are improved with PZQ treatment due to the liver injury and fibrosis being addressed, as well as the PZQ's action mechanisms, which are similar to those previously described (belonging to plant extracts) [45–47]. Conversely, liver damage is improved with *C. procera* extract, and inflammation is reduced, likely due to the extract's effect on the liver and fibrosis, as confirmed by evidence of increased serum markers [33]. This beneficial effect is likely due to *Calotropis* supporting the integrity of hepatocyte membranes and contributing to cell regeneration, thereby promoting normal levels of enzymes.

Regarding the hepatic apoptotic state, the *Schistosoma*-infected group showed disruption in the balance between pro-apoptotic and anti-apoptotic proteins (the *BAX*/Bcl-2 ratio), increasing *BAX* and decreasing Bcl-2, which shifts the liver environment toward apoptosis [46]. This misbalancing occurs due to chronic inflammation caused by the infection, which first activates the NF-κB and JNK signaling pathways, leading to the upregulation of *BAX* and downregulation of Bcl-2 expression [47,48]. Additionally, it increases ROS levels, which exacerbates mitochondrial membrane damage and enhances *BAX* translocation [49,50]. The *BAX*/Bcl-2 ratio is often considered a more informative prognostic marker than the individual expression levels of *BAX* or Bcl-2 alone [51]. In the present study, this ratio was significantly closer (decreased) to the optimal values (negative control group) in the plant extract- and silver nanoparticle-treated groups. In contrast, a study

stated that CpE increased *BAX* expression and reduced *Bcl-2* levels in HepG2 cells [52]. This can be explained by the presence of a relative difference in the effective phytochemicals of the applied plant extracts, attributed to the type of solvent (water *vs.* methanolic), the part of the plant used (stems *vs.* roots), and species (*C. procera vs. C. gigantea*), respectively. Furthermore, a study [53] reported that calotropin, a bioactive cardenolide isolated from Calotropis, leads to the upregulation of BAX/Bak1, accompanied by a significant reduction in Bcl-2 expression, in breast cancer patients. Generally, calotropin's pro-apoptotic effect, which involves increasing the BAX/Bcl-2 ratio, is well-documented in tumor models.

CpE has been shown to decrease apoptosis in liver cells of infected hosts, contributing to hepatoprotection. In *Plasmodium berghei*-infected mice, it was found that the treatment with *C. procera* leaf extract combined with biosynthesized silver nanoparticles significantly reduced liver histopathological damage and oxidative stress caused by infection, suggesting decreased liver cell apoptosis [54]. This indicates that plant extracts (such as *Calotropis*) may have contradictory physiological effects depending on the nature of the organisms (infected animal, tumor environment, or even healthy animals). Accordingly, different physiological pathways may be induced by the same plant extract in organisms with different physiological environments, or the plant extract may induce modifications in the dynamic equilibrium inside a specific physiological pathway. Regarding PZQ and hepatic apoptosis in this study, PZQ showed the lowest performance in normalizing apoptosis levels. Many studies have reported that PZQ, in schistosomiasis-infected animals, normalizes liver pathology by reducing inflammatory and apoptotic responses [55].

It was found that the murine kidney function was affected by the schistosomiasis infection. That fact was represented by the significant elevations in serum urea and creatinine levels, indicating a renal dysfunction. This dysfunction was attributed to the elevated levels of inflammatory cytokines, such as *TNF-α*, *IL-1β*, and *IL-6*, in response to the formation of granulomas. These cytokines intensify the production of ROS in renal tissues, leading to tissue damage, which is followed by the accumulation of urea and creatinine in the bloodstream [56].

The present study showed that PZQ was the most effective in reducing blood urea levels, followed by the plant extract. PZQ's effect on serum urea levels has been investigated in infected animals, with generally minimal impact on urea concentrations. In *S. mansoni*-infected mice, PZQ treatment reduced kidney pathology, with some restoration of normal renal function biomarkers, including serum urea; however, changes were not always statistically significant, depending on the dose and infection stage [57]. As in the results of the present study, CpE has been reported to affect serum urea/creatinine levels in infected organisms primarily through its nephroprotective and hepatoprotective actions, which help normalize kidney function disrupted by infection or toxicity [58,59]. This nephroprotective effect is attributed to the antioxidant activity, which reduces oxidative stress in renal tissues, and anti-inflammatory properties, which mitigate tissue damage. It is worth noting that high doses or small-sized silver NPs may cause renal stress or toxicity, reflected by increased serum urea and creatinine and histopathological kidney changes [60]. In contrast, the present GSNPs have shown positive effects on serum urea and creatinine levels in animals infected with *Schistosoma*. At low or moderate doses, GSNPs generally do not cause significant changes in serum urea or creatinine in healthy animals [61].

From this study, it is clear that the plant extracts outperformed PZQ in improving liver efficiency by supporting anti-fibrotic and antiapoptotic activities and reducing immune infiltration. The nanoparticles also exhibited the same anti-fibrotic effect on the liver; furthermore, they had the most significant improving effect on oxidative stress markers and antioxidant enzymes. On the other hand, although PZQ showed the highest antiparasitic effects (as indicated by the parasitic parameters), its physiological effects on the host were less pronounced in terms of oxidative stress markers, apoptosis, and antioxidant enzyme activities. Hence, it becomes clear that the actual evaluation of the three schistosomiasis protocols overlaps. Therefore, a comprehensive, objective evaluation of each protocol must be conducted by calculating the normalization percentages for each measured criterion, whether parasitic or host physiological, and then calculating the total efficacy of each protocol according to the equations mentioned in this study.

Conclusion

This study highlights the importance of assessing host liver and kidney function when evaluating antiparasitic treatments. *Calotropis procera* extract (200 mg/kg orally) and GSNPs (200 mg/kg intraperitoneally) both normalized the hepatic *BAX*/Bcl-2 ratio, indicating reduced apoptosis. Although GSH and MDA levels remained similar across treatments, the plant extract was more effective in lowering NO. Both treatments improved SOD and CAT activities, while PZQ and plant extract produced the greatest reductions in ALT, AST, and γ-GT. These findings support integrated evaluation of host physiology alongside parasitic endpoints. In general, determining the optimal treatment is challenging because each protocol involves variable factors, including nanoparticle size and vehicle, extract concentration and dose, and drug formulation. Regarding the solution to this problem, the present study established a mathematical technique that provides an overall

evaluation of anti-schistosomiasis protocols, considering not only the experiment's results but also the weight and importance of each measurement criterion in relation to the research objective. Additionally, it is essential to conduct multiple studies within each protocol separately, adjusting these variables to achieve a balanced therapeutic vision that considers both the more normalized physiological state of the host and the maximum anti-parasitic effect. In addition, future studies should integrate *in silico* approaches, including molecular docking and pharmacokinetic modeling, to predict probable interactions between silver nanoparticles, plant phytochemicals, and parasite targets. This computational insight can guide nanoparticle design, optimize dosing regimens, and elucidate mechanistic pathways, thereby strengthening the translational potential of green silver therapies.

List of abbreviations

ALT, Alanine transaminase; AST, Aspartate transaminase; *BAX*, Bcl2-cell-associated X protein; Bcl-2, B-cell lymphoma protein 2; CAT, Catalase; CpE, *Calotropis procera* extract; DLS, Dynamic light scattering; FTIR, Fourier transform infrared spectroscopy; GSH, Reduced glutathione; GSNPs, Green-silver nanoparticles; γ-GT, Gamma-glutamyl transferase; JNK, c-Jun N-terminal Kinase; MDA, Malondialdehyde; NF-κB, Nuclear Factor kappa-light-chain-enhancer of activated B cells; NPs, Nanoparticles; NO, Nitric oxide; PZQ, Praziquantel; SBSC, Schistosome Biology Supply Center; SOD, Superoxide dismutase; TWB, Total worm burden.

Acknowledgment

The authors extend their appreciation to the technicians of the Theodor Bilharz Institute, Cairo, Egypt, for their efforts in animal care. The authors received no financial support for the research and authorship.

Conflicts of interest

The authors declare that they have no known competing financial interests or personal relationships that could have appeared to influence the work reported in this paper.

Authors' contributions

ZKH: Resources, Methodology, Conceptualization. MFN and NAM: Resources, Visualization, Conceptualization. MIS: Supervision, Visualization. MAA: Writing - Review & Editing, Formal analysis, Methodology (Physiological study). AHN: Writing—Original Draft, Writing—Review & Editing, Methodology (Histological study).

References

[1] El Ridi R, Tallima H, Dalton JP, Donnelly S. Induction of protective immune responses against schistosomiasis using functionally active cysteine peptidases. Front Genet 2014; 5:119; https://doi.org/10.3389/fgene.2014.00119

[2] Mengarda AC, Iles B, F. Longo JP, De Moraes J. Recent trends in praziquantel nanoformulations for helminthiasis treatment. Expert Opinion Drug Del 2022; 19(4):383–93; https://doi.org/10.1080/17425247.2022.2051477

[3] Malhab LJB, Bajbouj K, Shehab NG, Elayoty SM, Sinoj J, Adra S, et al. Potential anticancer properties of *Calotropis procera*: an investigation on breast and colon cancer cells. Heliyon 2023; 9(6):e16706; https://doi.org/10.1016/j.heliyon.2023.e16706

[4] Abbas M, Arshad M, Rafique MK, Altalhi AA, Saleh DI, Ayub MA, et al. Chitosan-polyvinyl alcohol membranes with improved antibacterial properties contained *Calotropis procera* extract as a robust wound healing agent. Arab J Chem 2022; 15(5):103766; https://doi.org/10.1016/j.arabjc.2022.103766

[5] Hamdan ZK, Soliman MI, Taha HA, Khalil MMH, Nigm AH. Antischistosomal effects of green and chemically synthesized silver nanoparticles: *in vitro* and *in vivo* murine model. Acta Trop 2023; 244:106952; https://doi.org/10.1016/j.actatropica.2023.106952

[6] Rani R, Sharma D, Chaturvedi M, Yadav JP. Phytochemical analysis, antibacterial and antioxidant activity of *Calotropis procera* and *Calotropis gigantea*. Nat Prod J 2019; 9(1):47–60; https://doi.org/10.2174/2210315508666180608081407

[7] Nigm A, Abou-Eldahab M, Khalil L, Juroud R, Azzam A, Taha H, et al. Ameliorative effect of *Calotropis procera* and/or Praziquantel on *Schistosoma mansoni* infected mice. J Egypt Soc Parasitol 2019; 49(3):529–38; https://doi.org/10.21608/JESP.2019.68055

[8] Moustafa MA, Mossalem HS, Sarhan RM, Abdel-Rahman AA, Hassan EM. The potential effects of silver and gold nanoparticles as molluscicides and cercaricides on *Schistosoma mansoni*. Parasitol Res 2018; 117:3867–80; https://doi.org/10.1007/s00436-018-6093-2

[9] Dkhil MA, Thagfan FA, Morad MY, Al-Shaebi EM, Elshanat S, Bauomy AA, et al. Biosynthesized silver nanoparticles have anticoccidial and jejunum-protective effects in mice infected with *Eimeria papillata*. Environ Sci Pollut Res Int 2023; 30(15):44566–77; https://doi.org/10.1007/s11356-023-25383-0

[10] Zhang P, Gong J, Jiang Y, Long Y, Lei W, Gao X, et al. Application of silver nanoparticles in parasite treatment. Pharmaceutics 2023; 15(7):1783; https://doi.org/10.3390/pharmaceutics15071783

[11] Siddiqa A, Qureshi R, Raja NI, Khan IA, Ahmad MZ, Rafique S, et al. Liver-boosting potential: chicory compound-mediated silver nanoparticles for hepatoprotection-biochemical and histopathological insights. Front Pharmacol 2024; 15:1325359; https://doi.org/10.3389/fphar.2024.1325359

[12] Shakib P, Zivdari M, Khalaf AK, Marzban A, Ganjalikhani-Hakemi M, Parvaneh J, et al. Nanoparticles as potent agents for treatment of *Schistosoma* infections: a systematic review. Curr Ther Res 2023; 99:100715; https://doi.org/10.1016/j.curtheres.2023.100715

[13] Ameta R, Rai AK, Vyas S, Bhatt JP, Ameta SC. Green synthesis of nanocomposites using plant extracts and their applications. Handb Greener Synth Nanomater Compd 2021; 1:663–82; https://doi.org/10.1016/b978-0-12-821938-6.00020-7

[14] Sikdar D, Roy K, Das B, Debnath SC. A novel green biosynthesis of superfine tin dioxide nanoparticle from *Ficus elastica* fallen leaf extract and exploring its suitability as green nano-filler for advancement of natural rubber composite. J Polym Res 2023; 30:346; https://doi.org/10.1007/s10965-023-03725-3

[15] Awad MA, Al Olayan EM, Siddiqui MI, Merghani NM, Alsaif SSA, Aloufi AS. Antileishmanial effect of silver nanoparticles: green synthesis, characterization, *in vivo* and *in vitro* assessment. Biomed Pharmacother 2021; 137:111294; https://doi.org/10.1016/j.biopha.2021.111294

[16] Al-Haid SF, Meligy AMA, Abdel-Raheem SM, Elalfy M, Elmadawy MA. Phytochemical profiling, bioactive compound isolation, and animal health implications of *Calotropis procera* in Al-Ahsa, Saudi Arabia. Open Vet J 2025; 15(6):2722; https://doi.org/10.5455/ovj.2025.v15.i6.41

[17] Nagime PV, Singh S, Shaikh NM, Gomare KS, Chitme H, Abdel-Wahab BA, et al. Biogenic fabrication of silver nanoparticles using *Calotropis procera* flower extract with enhanced biomimetics attributes. Materials 2023; 16(11):4058; https://doi.org/10.3390/ma16114058

[18] Nazeer W, Hassanein E, Barakat N. Green synthesis of silver nanoparticles using *Caltropis procera* and *Amaranthus ascendens* stem extracts and evaluation of their antimicrobial activity. Afr J Biol Sci 2023; 19(1):53–67; https://doi.org/10.21608/ajbs.2023.194290.1052

[19] Malabade R, Taranalli A. *Calotropis procera*: a potential cognition enhancer in scopolamine and electroconvulsive shock-induced amnesia in rats. Indian J Pharmacol 2015; 47(4):419–24; https://doi.org/10.4103/0253-7613.161269

[20] Duvall RH, Dewitt WB. An improved perfusion technique for recovering adult schistosomes from laboratory animals. Am J Trop Med Hyg 1967; 16(4):483–6; https://doi.org/10.4269/ajtmh.1967.16.483

[21] Pellegrino J, Oliveira CA, Faria J, Cunha AS. New approach to the screening of drugs in experimental schistosomiasis mansoni in mice. Am J Trop Med Hyg 1962; 11(2):201–15; https://doi.org/10.4269/ajtmh.1962.11.201

[22] Kamel IA, Cheever AW, Elwi AM, Mosimann JE, Danner R. *Schistosoma mansoni* and S. haematobium infections in Egypt. I. Evaluation of techniques for recovery of worms and eggs at necropsy. Am J Trop Med Hyg 1977; 26(4):696–701; https://doi.org/10.4269/ajtmh.1977.26.696

[23] Hussein A, Rashed S, El Hayawan I, El-Sayed R, Ali H. Evaluation of the anti-schistosomal effects of turmeric (*Curcuma longa*) versus praziquantel in *Schistosoma mansoni*-infected mice. Iran J Parasitol 2017; 12:587–96.

[24] Yepes E, Varela-M RE, López-Abán J, Rojas-Caraballo J, Muro A, Mollinedo F. Inhibition of granulomatous inflammation and prophylactic treatment of schistosomiasis with a combination of edelfosine and praziquantel. PLoS Negl Trop Dis 2015; 9:3893; https://doi.org/10.1371/journal.pntd.0003893

[25] Yoshioka T, Kawada K, Shimada T, Mori M. Lipid peroxidation in maternal and cord blood and protective mechanism against activated-oxygen toxicity in the blood. Am J Obstet Gynecol 1979; 135(3):372–6; https://doi.org/10.1016/0002-9378(79)90708-7

[26] Montgomery HAC, Dymock JE. The determination of nitrite in water. Analyst 1961; 86:414–6; https://doi.org/10.1039/an9618600016

[27] Nishikimi M, Rao NA, Yagi K. The occurrence of superoxide anion in the reaction of reduced phenazine methosulphate and molecular oxygen. Biochem Biophys Res Commun 1972; 46(2):849–54; https://doi.org/10.1016/S0006-291X(72)80218-3

[28] Aebi H. Catalase *in vitro*. Methods Enzymol 1984; 105:121–6; https://doi.org/10.1016/S0076-6879(84)05016-3

[29] Beutler E, Duron O, Kelly BM. Improved method for the determination of blood glutathione. J Lab Clin Med 1963; 61:882–8.

[30] Eltaly RI, Baz MM, Radwan IT, Yousif M, Abosalem HS, Selim A, et al. Novel acaricidal activity of *Vitex castus* and *Zingiber officinale* extracts against the camel tick, *Hyalomma dromedarii*. Int J Vet Sci 2023; 12(2):255–9; https://doi.org/10.47278/journal.ijvs/2022.184

[31] Cascone S, Lamberti G, Barba AA. Size characterization of natural nanoparticles: different techniques for different applications. Curr Opin Food Sci 2021; 40:99–106.

[32] Carri MT, Valle C, Bozzo F, Cozzolino M. Oxidative stress and mitochondrial damage: importance in non-SOD1 ALS. Front Cell Neurosci 2015; 9:41; https://doi.org/10.3389/fncel.2015.00041

[33] Sombié EN, Traoré TK, Derra AN, N'do JYP, Belem-Kabré WLM, Ouédraogo N, et al. Anti-fibrotic effects of *Calotropis procera* (Ait.) R.Br roots bark against diethylnitrosamine-induced hepatic fibrosis in rats. J Biosci Med 2023; 11(4):332–49; https://doi.org/10.4236/jbm.2023.114024

[34] Roehlen N, Crouchet E, Baumert TF. Liver fibrosis: mechanistic concepts and therapeutic perspectives. Cells 2020; 9(4):875; https://doi.org/10.3390/cells9040875

[35] Mallat A, Lotersztajn S. Fibrose hépatique: de la physiopathologie aux implications thérapeutiques. Gastroenterol Clin Biol 2009; 33(8-9):789–98; https://doi.org/10.1016/j.gcb.2009.05.004

[36] Hong J, Jin H, Han J, Hu H, Liu J, Li L, et al. Infusion of human umbilical cord derived mesenchymal stem cells effectively relieves liver cirrhosis in DEN-induced rats. Mol Med Rep 2014; 9:1103–11; https://doi.org/10.3892/mmr.2014.1927

[37] Sun X, Wang Z, Zhai S, Cheng Y, Liu J, Liu B. *In vitro* cytotoxicity of silver nanoparticles in primary rat hepatic stellate cells. Mol Med Rep 2013; 8(5):1365–72; https://doi.org/10.3892/mmr.2013.1683

[38] Diallo F, Seck I, Ndoye SF, Niang T, Dieng SM, Thiam F, et al. Green synthesis and anti-inflammatory activity of silver nanoparticles based on leaves extract of *Aphania senegalensis*. Biochem Res Int 2024; 2024:3468868; https://doi.org/10.1155/2024/3468868

[39] Guzzatti MFM, De Moura AB, Venturini LM, De Roch Casagrande L, Lima IR, Da Costa C, et al. Biosynthesized silver nanoparticles modulate inflammation in a palatine wound model. Clin Exp Dent Res 2025; 11(5):e70213; https://doi.org/10.1002/cre2.70213

[40] Zhang H, Jacob JA, Jiang Z, Xu S, Sun K, Zhong Z, et al. Hepatoprotective effect of silver nanoparticles synthesized using aqueous leaf extract of *Rhizophora apiculata*. Int J Nanomed 2019; 14:3517–24; https://doi.org/10.2147/IJN.S198895

[41] Karunakar KK, Cheriyan BV, Babu D, Devan P, Nandhini J, Kannan MS, et al. Selenium, silver, and gold nanoparticles: emerging strategies for hepatic oxidative stress and inflammation reduction. Nano Trans Med 2025; 4:100085; https://doi.org/10.1016/j.ntm.2025.100085

[42] Dos Santos VHB, De Azevedo Ximenes ECP, De Souza RAF, Da Silva RPC, Da Conceição Silva M, De Andrade LVM, et al. Effects of the probiotic *Bacillus cereus* GM on experimental *Schistosomiasis mansoni*. Parasitol Res 2024; 123:72; https://doi.org/10.1007/s00436-023-08090-0

[43] Liang YJ, Luo J, Yuan Q, Zheng D, Liu YP, Shi L, et al. New insight into the antifibrotic effects of praziquantel on mice in infection with *Schistosoma japonicum*. PLoS One 2011; 6(5):e20247; https://doi.org/10.1371/journal.pone.0020247

[44] Liu J, Kong D, Qiu J, Xie Y, Lu Z, Zhou C, et al. Praziquantel ameliorates CCl_4-induced liver fibrosis in mice by inhibiting TGF-β/Smad signalling via up-regulating Smad7 in hepatic stellate cells. Br J Pharmacol 2019; 176(24):4666–80; https://doi.org/10.1111/bph.14831

[45] Niu X, Hu T, Hong Y, Li X, Shen Y. The role of praziquantel in the prevention and treatment of fibrosis associated with Schistosomiasis: a review. J Trop Med 2022; 2022:1413711; https://doi.org/10.1155/2022/1413711

[46] Zhao J, Liu X, Chen Y, Zhang LS, Zhang YR, Ji DR, et al. STAT3 promotes schistosome-induced liver injury by inflammation, oxidative stress, proliferation, and apoptosis signal pathway. Infect Immun 2021; 89(3):10; https://doi.org/10.1128/iai.00309-20

[47] Lee SY, Le DD, Bae CS, Park JW, Lee M, Cho SS, et al. Oleic acid attenuates asthma pathogenesis via Th1/Th2 immune cell modulation, TLR3/4-NF-κB-related inflammation suppression, and intrinsic apoptotic pathway induction. Front Immunol 2024; 15:1429591; https://doi.org/10.3389/fimmu.2024.1429591

[48] Rozik OI, Hussein MM, El-Elebiarie AS, Nady S. *In vitro* anti-inflammatory activity of bee venom melittin and phospholipase A_2 on murine splenocytes stimulated with *Schistosoma mansoni* antigens. Egypt Acad J Biol Sci C Physiol Mol Biol 2024; 16(2):75–88; https://doi.org/10.21608/eajbsc.2024.371726

[49] Lu JL, Yu CX, Song LJ. Programmed cell death in hepatic fibrosis: current and perspectives. Cell Death Discovery 2023; 9:449; https://doi.org/10.1038/s41420-023-01749-8

[50] Xiang F, Zhang Z, Li Y, Li M, Xie J, Sun M, et al. Research progress in the treatment of schistosomiasis with traditional Chinese medicine. J Ethnopharmacol 2024; 333:118501; https://doi.org/10.1016/j.jep.2024.118501

[51] Kulsoom B, Shamsi TS, Afsar NA, Memon Z, Ahmed N, Hasnain SN. BAX, Bcl-2, and BAX/Bcl-2 as prognostic markers in acute myeloid leukemia: are we ready for Bcl-2-directed therapy? Cancer Manag Res 2018; 10:403–16; https://doi.org/10.2147/CMAR.S154608

[52] Priya V, Jain P, Vanathi BM, Raj PV, Kamath BV, Rao JV, et al. Methanolic root extract of *Calotropis gigantea* induces apoptosis in human hepatocellular carcinoma by altering BAX/Bcl-2 expression. Am J Pharmacol Sci 2015; 3(1):13–7.

[53] Rajkovic J, Novakovic R, Grujic-Milanovic J, Ydyrys A, Ablaikhanova N, Calina D, et al. An updated pharmacological insight into calotropin as a potential therapeutic agent in cancer. Front Pharmacol 2023; 14:1160616; https://doi.org/10.3389/fphar.2023.1160616

[54] Murshed M, Al-Tamimi J, Mares M, Hailan W, Ibrahim K, Al-Quraishy S. Pharmacological effects of biosynthesis silver nanoparticles utilizing *Calotropis procera* leaf extracts on *Plasmodium berghei*-infected liver in experiment mice. Int J Nanomed 2024; 19:13717–3; https://doi.org/10.2147/IJN.S490119

[55] Mccusker P, Rohr CM, Chan JD. *Schistosoma mansoni* alter transcription of immunomodulatory gene products following *in vivo* praziquantel exposure. PLoS Negl Trop Dis 2021; 15(3):9200; https://doi.org/10.1371/journal.pntd.0009200

[56] Ali SB, Mohamed AS, Fahmy SR, El–Garhy M, Mousa MR, Abdel-Ghaffar F. Anthelmintic and hepatoprotective activities of the green-synthesized zinc oxide nanoparticles against *Parascaris equorum* infection in rats. Acta Parasit 2024; 69:283–301; https://doi.org/10.1007/s11686-023-00728-4

[57] El-Wakil ES, Tolba MM, El-Sayad MH, Khairy Hassen M, Al-Rashidi HS, Almayouf MA, et al. A comparative parasitological, histopathological, and proteomic analysis of *Schistosoma mansoni*-infected mice treated with ivermectin and praziquantel. Front Vet Sci 2025; 12:1646155; https://doi.org/10.3389/fvets.2025.1646155

[58] Dahiru D, Amos A, Sambo SH. Effect of ethanol extract of *Calotropis procera* root bark on carbon tetrachloride-induced hepatonephrotoxicity in female rats. Jordan J Biol Sci 2013; 6(3):227–30; https://doi.org/10.12816/0001538

[59] Javed S. Experimental evaluation of nephroprotective potential of *Calotropis procera* (Ait) flowers against gentamicin-induced toxicity in albino rabbits. Pak Vet J 2015; 35(2):222–6.

[60] Salama B, Alzahrani KJ, Alghamdi KS, Al-Amer O, Hassan KE, Elhefny MA, et al. Silver nanoparticles enhance oxidative stress, inflammation, and apoptosis in liver and kidney tissues: potential protective role of thymoquinone. Res Sq 2022; v1:1–22; https://doi.org/10.21203/rs.3.rs-1828575/v1

[61] Barabadi H, Noqani H, Soltani M, Kashani AS. Animal-based evidence supports protective activity of bioengineered silver and gold nanomaterials on hepatic and renal function profile parameters. Front Nanotechnol 2025; 6:1424562; https://doi.org/10.3389/fnano.2024.1424562

Supplementary Material

Table 1. Effect of CpE, Green AgNPs, and PZQ on the hepatic oxidative stress markers: reduced GSH, MDA, and NO in the experimental groups.

Groups	GSH (mg/mg)	MDA (µm/mg)	NO (µm/mg)
Control	1.94 ± 0.03	25.92 ± 3.88	11.26 ± 0.7
Infected	1.527 ± 0.07[a]	51.5 ± 4.6[a]	58.47 ± 6.13[a]
Infected + PZQ	1.82 ± 0.02[b]	31.24 ± 3.97[b]	28.09 ± 6.32[b]
Infected + CPE	2.05 ± 0.05[b]	25.24 ± 3.91[b]	15.9 ± 3.69[b]
Infected + GSNP	2.31 ± 0.02[b]	21.29 ± 5.6[b]	19.61 ± 4.71[b]

- Results expressed as Mean ± SEM.
- ANOVA was first applied,
- Tukey's test for multiple comparisons was used for multiple comparisons; $p < 0.05$ is regarded as significant.
- [a] significant difference versus control (infected *vs.* control), [b] Significant difference versus infected value.

Table 2. Effect of CpE, Green AgNPs, and PZQ on the hepatic protein concentration of BAX and Bcl-2 in the experimental groups.

Groups	BAX (pg/mg)	Bcl-2 (pg/mg)
Control	42.615 ± 3.9	153.59 ± 5.95
Infected	61.54 ± 3.24[b]	105.83 ± 9.88[a]
Infected + PZQ	48.38 ± 3.58[b]	139.31 ± 6.38[b]
Infected + CPE	31.49 ± 3.43[bc]	133.19 ± 1.95[b]
Infected + GSNP	40.2 ± 3.12[b]	132.22 ± 2.1[b]

- Results expressed as Mean ± SEM.
- ANOVA was first applied,
- Tukey's test for multiple comparisons was used for multiple comparisons; $p < 0.05$ is regarded as significant.
- [a] significant difference versus control (infected *vs.* control), [b] Significant difference versus infected value.

Table 3. The sera levels of ALT, AST, and γ-GT in the experimental groups.

Groups	ALT (U/l)	AST (U/l)	γ-GT (U/l)
Control	19.75 ± 1.65	18.75 ± 1.70	2.80 ± 0.26
Infected	92.50 ± 1.93[a]	95.50 ± 1.93[a]	24.27 ± 1.02[a]
Infected + PZQ	33.25 ± 1.65[b]	34.50 ± 1.84[b]	8.45 ± 0.28[b]
Infected + CPE	44.25 ± 2.56[b]	42.50 ± 0.95[b]	9.20 ± 0.17[b]
Infected + GSNP	66.25 ± 2.56[b]	62.75 ± 1.37[b]	15.45 ± 0.96[b]

- Results expressed as Mean ± SEM.
- ANOVA was first applied,
- Tukey's test for multiple comparisons was used for multiple comparisons; $p < 0.05$ is regarded as significant.
- [a] significant difference versus control (infected *vs.* control), [b] Significant difference versus infected value.

Table 4. Effect of CpE, Green AgNPs, and PZQ on hepatic antioxidant enzyme activities SOD and CAT in experimental groups.

Groups	SOD (U/mg)	CAT (U/mg)
Control	75.68 ± 4.22	0.65 ± 0.071
Infected	36.12 ± 4.52[a]	0.39 ± 0.013[a]
Infected + PZQ	45.88 ± 6.37[a]	0.46 ± 0.07[b]
Infected + CPE	61.57 ± 6.02[b]	0.59 ± 0.008[b]
Infected + GSNP	60.77 ± 5.61[b]	0.61 ± 0.01[b]

- Results expressed as Mean ± SEM.
- ANOVA was first applied,
- Tukey's test for multiple comparisons was used for multiple comparisons; $p < 0.05$ is regarded as significant.
- [a] significant difference versus control (infected *vs.* control), [b] Significant difference versus infected value.

Table 5. The serum levels of urea and creatinine in experimental groups.

Groups	Urea (mg%)	Creatinine (mg%)
Control	28.00 ± 1.47	0.67 ± 0.025
Infected	56.50 ± 1.19[a]	1.70 ± 0.070[a]
Infected + PZQ	32.75 ± 1.54[b]	0.98 ± 0.011[b]
Infected + CPE	39.50 ± 0.64[b]	1.00 ± 0.040[b]
Infected + GSNP	48.00 ± 0.91[b]	1.47 ± 0.025[b]

- Results expressed as Mean ± SEM.
- ANOVA was first applied,
- Tukey's test for multiple comparisons was used for multiple comparisons; $p < 0.05$ is regarded as significant.
- [a] significant difference versus control (infected *vs.* control), [b] Significant difference versus infected value.